IEEE Photonics Journal
An IEEE Photonics Society Publication

Open Access

Reconfigurable Electro-optic Logic Circuits Using Microring Resonator-Based Optical Switch Array

Volume 8, Number 2, April 2016

Yonghui Tian
Guolin Zhao
Zilong Liu
Anqi Guo
Huifu Xiao
Xiaosuo Wu
Yinghao Meng
Lin Deng
Xiaonan Guo
Guipeng Liu
Jianhong Yang

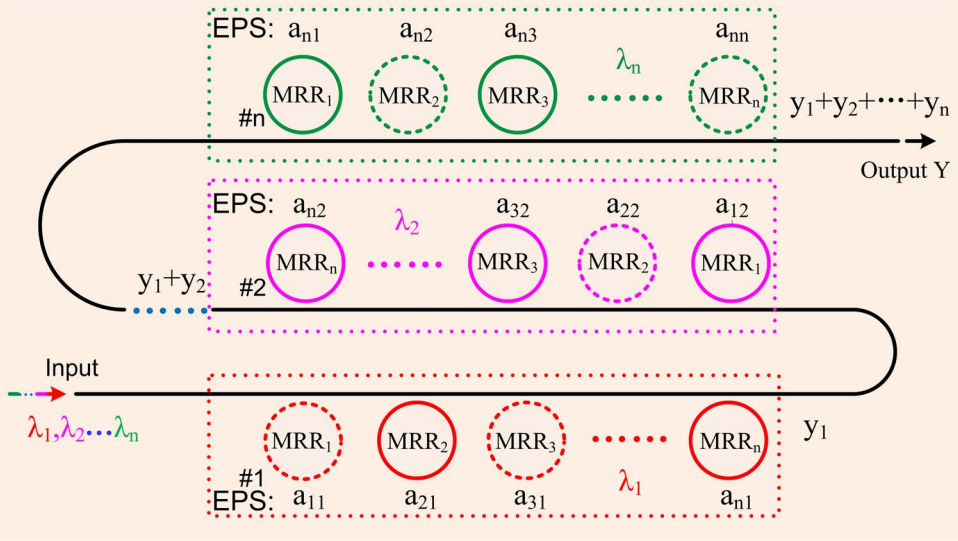

DOI: 10.1109/JPHOT.2016.2524009
1943-0655

Reconfigurable Electro-optic Logic Circuits Using Microring Resonator-Based Optical Switch Array

Yonghui Tian, Guolin Zhao, Zilong Liu, Anqi Guo, Huifu Xiao, Xiaosuo Wu, Yinghao Meng, Lin Deng, Xiaonan Guo, Guipeng Liu, and Jianhong Yang

Institute of Microelectronics and Key Laboratory for Magnetism and Magnetic Materials of Ministry of Education, School of Physical Science and Technology, Lanzhou University Lanzhou 730000, China

DOI: 10.1109/JPHOT.2016.2524009

Manuscript received November 25, 2015; revised January 24, 2016; accepted January 27, 2016. Date of publication February 2, 2016; date of current version February 22, 2016. This work was supported in part by the National Science Foundation of China under Grant 61405082, by the Natural Science Foundation of Gansu Province under Grant 145RJZA110, and by the Fundamental Research Funds for the Central Universities. Corresponding author: Y. Tian (e-mail: Siphoton@lzu.edu.cn).

Abstract: In this paper, we propose a reconfigurable electro-optic logic circuit, which can perform any combinatorial logic operations using a microring resonator (MRR)-based optical switching array. The operands are represented by electrical signals, which are applied to the corresponding MRRs to control their switching status. The operation results are directed to the output port in the form of light. For proof of concept, the circuit consisting of four thermooptic MRR-based optical switches is fabricated on the silicon-on-insulator (SOI) substrate using the commercial complementary metal–oxide–semiconductor (CMOS) fabrication process. Finally, several logic operations of four operands with the operation speed of 10 kb/s are demonstrated successfully.

Index Terms: Integrated optics, optical switching devices, optical logic devices, resonators, photonic integrated circuits.

1. Introduction

Electro-optic logic is a novel paradigm which employs electrical signal to control the optical switches status in the optical switch array (or the optical switch network) to perform the logic operations, and the operation results are in the form of light. The status of each optical switch in the optical switch array is determined by an electrical Boolean signal applied to it. The operation of each optical switch is independent of other optical switches in the array and the operation results propagate in the array circuit at the speed of light. The overall latency of the logic circuit is very small, and all optical switches perform their operations almost simultaneously. Therefore, the electro-optic logic circuit has higher operation speed and lower latency [1]–[6]. In addition, it is exciting that the control signal is electron and the operation signal is photon in the electro-optic logic scheme. The electrical signal is easily controlled and optical signal is more appropriate as operation signal due to its nature features such as high propagation speed, parallel operation, high bandwidth, etc. Therefore, electro-optic logic utilizes the advantages of electron and photon while avoiding their drawbacks.

Recently, many electro-optic logic circuits have been proposed and demonstrated [6]–[9], and the operation speed of electro-optic logic circuits has been up to 20 Gbps [9]. However, they

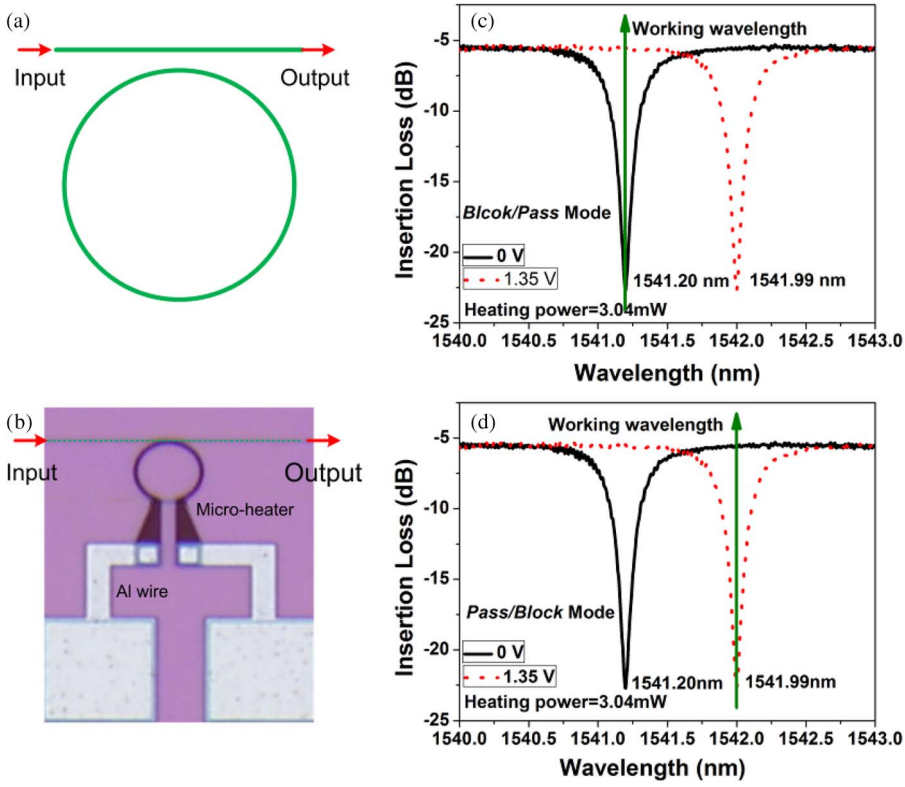

Fig. 1. (a) Single MRR with one waveguide, (b) the optical switch consisting of a single MRR and one waveguide, (c) the transmission spectra of the optical switch in block/pass mode (the status of the optical switch is from OFF to ON), and (d) the transmission spectra of the switch in pass/block mode (the status of the optical switch is from ON to OFF).

only can perform one or several specific logic operations, which undoubtedly limit their practical applications in the future. Indeed, one kind of reconfigurable electro-optic logic circuit based on the optical switch networks has been proposed and demonstrated recently, and the reconfigurable electro-optic logic circuits can perform any combinatorial logic operations according to the truth tables of logic functions [10], [11]. However, the Multiplexer (MUX) and Demultiplexer (DEMUX) elements are included in the logic circuit in [8], which increases the complexities of the logic circuit. In this paper, we propose and demonstrate another reconfigurable electro-optic logic circuit which can perform any combinatorial logic operations according to the logic expressions using MRR-based optical switch array. For the proposed logic circuit, the MUX/DEMUX elements are integrated with computing elements, which means the MUX/DEMUX and logic operation function are achieved by the proposed logic circuit simultaneously. In other words, the proposed logic circuit does not need additional MRRs to achieve MUX/DEMUX function. Therefore, it is more compact than that in [10].

2. Device Working Principle, Design, and Fabrication

As we know, any logic functions can be expressed as the sum of a number of terms, and each term is the product of a number of variables [11]. For example, any logic function Y can be expressed as $Y = y_1 + y_2 + \cdots + y_n$, and y_n denotes the product of a number of variables, such as $y = \bar{a}_1 a_2 \bar{a}_3 \cdots a_n$ ($\bar{a}_n$ represents the opposite logic value of a_n). According to the logic expression, we propose a reconfigurable electro-optic logic circuit which can perform any combinatorial logic operations based on MRR-based optical switch array. MRR-based optical switch consisting of a single MRR and one waveguide is shown in Fig. 1(a), which is a fundamental building

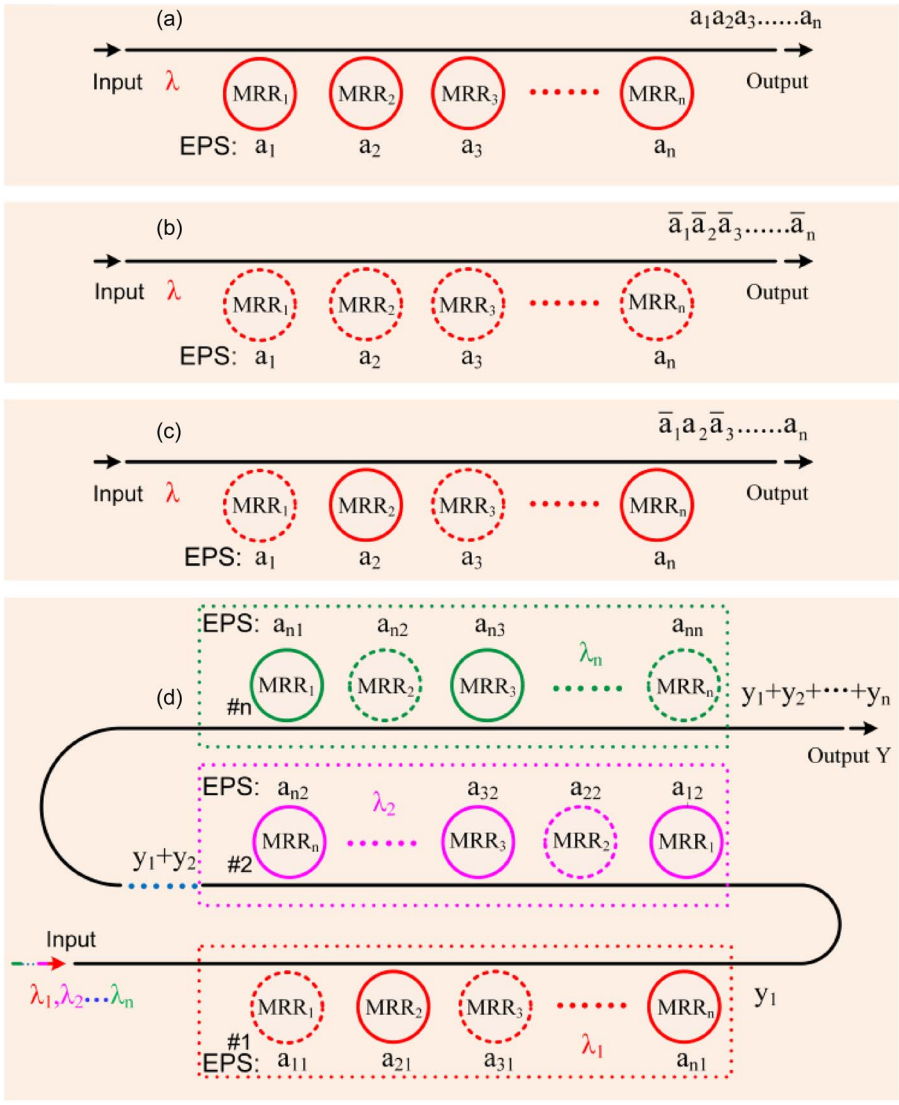

Fig. 2. Logic circuit with (a) one working wavelength and all MRRs work in the block/pass mode, (b) one working wavelength and all MRRs work in the pass/block mode, (c) one working wavelength and MRRs working in the pass/block or block/pass mode, and (d) the proposed reconfigurable logic circuit. The solid line ring denotes MRR works in the block/pass mode, the dot line ring denotes MRR works in the pass/block mode, MRRs with the same color work at the same working wavelength. EPS: electrical pulse sequences.

block for the proposed reconfigurable logic circuit. The micrograph of the optical switch consisting of a single MRR and one waveguide is shown in Fig. 1(b). The electrical signal applied to MRR through the micro-heater is employed to control the working status of the optical switch.

Generally speaking, there are two different operation modes for each optical switch: *block/pass* and *pass/block* modes. Each switch is in either the *block/pass* or the *pass/block* mode depending on the voltage applied to it. The MRR switch which works in *block/pass* mode is on-resonance at the working wavelength when the applied voltage is 0 V (logic 0) and off-resonance when the voltage is 1.35 V (logic 1) (see Fig. 1(c)). The *pass/block* mode is just the opposite (see Fig. 1(d)). In Fig. 1(a), the input single wavelength optical signal will be dropped by MRR when MRR is on-resonance or directed to the output port when MRR is off-resonance.

The proposed logic circuit is composed of N MRRs and one waveguide (see Fig. 2(d)). In fact, the architecture of the logic circuit is the optical switch array consisting of N MRR-based optical

switches. In order to explain the operation principle of the proposed logic circuit more simply, we first explain the operation principles of Fig. 2(a)–(c). A monochromatic continuous light with the working wavelength of λ is coupled into the input port of logic circuits (see Fig. 2(a)–(c)) and then modulated by the electrical pulse sequences (EPS) $a_1, a_2, a_3, \ldots, a_n$ applied to $MRR_1, MRR_2, MRR_3, \ldots, MRR_n$, respectively. The low and high levels of EPS represent logic 0 and logic 1 in electrical domain, respectively; the low and high levels of the optical power at the output port represent logic 0 and logic 1 in optical domain, respectively. As we known, as long as one of all MRRs is on-resonance in Fig. 2(a), the light transmitted in the straight waveguide is blocked. Therefore, the optical power at the output port is at low level, and logic 0 is achieved at the output port. Based on the above discussions about the operation modes of MRR-based optical switches, we define the operation modes of all MRRs as the *block/pass* mode. As long as one of N operands $(a_1, a_2, a_3, \ldots, a_n)$ is logic 0, or one of all MRRs is on-resonance; therefore, the light transmitted in the straight waveguide is blocked. The optical power is at low level, and logic 0 is achieved at the output port. Therefore, the logic circuit of Fig. 2(a) can perform the AND operation of N operands. The operation result y can be expressed as $y = a_1 a_2 a_3 \cdots a_n$. Similarly, if all MRRs work in the *pass/block* mode, the logic circuit can perform the AND operation of N inverse operands. The operation result can be expressed as $y = \bar{a}_1 \bar{a}_2 \bar{a}_3 \cdots \bar{a}_n$ (Fig. 2(b)). If some MRRs work in the *pass/block* mode and other MRRs work in the *block/pass* mode, the logic circuit can also perform the AND operation of N operands. However, some inverse operands are included in the N operands in this working status in this case. For example, we define MRR_1 and MRR_3 work in the *pass/block* mode and the other MRRs work in the *block/pass* mode in Fig. 2 (c). The operation result y can be expressed as $y = \bar{a}_1 a_2 \bar{a}_3 \cdots a_n$. In a word, if the continuous wave coupled into the logic circuit is monochromatic; the product of any N variables can be achieved at the output port in the form of light according to the definitions of MRR different operation modes. Wavelength division multiplexing (WDM) technology can also be employed to achieve reconfigurable logic operation in here (see Fig. 2(d)). Multi-wavelength signal lights with the wavelength of $\lambda_1, \lambda_2, \ldots, \lambda_n$ are coupled into the input port simultaneously. MRRs in the logic circuit are divided into different groups, all MRRs in one group work at the same wavelength. Based on the above discussions, every group can perform the product of any variables. The operation results of all groups are multiplexed together at last. Therefore, the final operation result Y can be expressed as $Y = y_1 + y_2 + \cdots + y_n$ (y_n denotes the product of any variables as shown in Fig. 2(d). Note that the numbers of groups are equal to the numbers of the working wavelengths, and the numbers of operands in every term are equal to the numbers of MRRs in every corresponding group. The proposed logic circuit is similar with the field programmable gate array (FPGA), and the resonance wavelengths of unused MRRs can be shifted to be far from the working wavelengths of the circuit through thermal tuning.

For a proof of principle, a reconfigurable electro-optic logic circuit based on four thermo-optic tunable MRRs is fabricated on an 8-inch silicon-on-insulator (SOI) wafer with a 220 nm top silicon layer and a 2 μm buried silicon dioxide layer, which can perform any logic operations of four operands. In here, the thermo-optic modulating scheme is adopted for the proof of principle since it demands a less complex device layer structure and consequently yields easier fabrication steps. Two-hundred forty eight-nanometer deep UV photolithography is used to define the device pattern and an inductively coupled plasma etching process is used to etch the top silicon layer. Compared to the strip waveguide with similar dimensions, the rib waveguide has less sidewall area which can reduce the scattering loss on the waveguide sidewall and thus the transmission loss is less than the strip waveguide with similar dimensions and a similar fabrication process [12]. Therefore, the bus and ring waveguides are formed by a submicron rib waveguide with a width of 400 nm, a height of 220 nm, and a slab thickness of 70 nm, and the mode performance of waveguide is shown in Fig. 3(a). From Fig. 3(a), we can see the higher-order modes are cutoff except for the quasi-TE fundamental mode when the waveguide width is 400 nm (the quasi-TE fundamental mode of the waveguide is shown in inset in Fig. 3(a), waveguide height: 220 nm, slab thickness: 70 nm). Therefore, numerical calculation shows that the waveguide only supports a quasi-TE fundamental mode (see Fig. 3(a)), which agrees with the

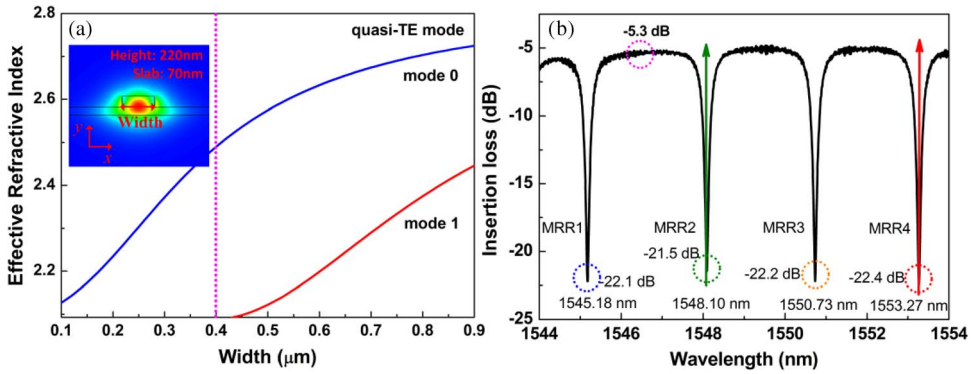

Fig. 3. (a) Mode performance of waveguide (the inset in Fig. 3(a) is the quasi-TE fundamental mode of waveguide). (b) Static response spectral of the device with no voltage applied to MRRs.

experimental results [7]. The radii of four MRRs are designed to be and 10.00 μm, 10.03 μm, 10.06 μm, and 10.09 μm in order to let four MRRs have slightly different initial resonance wavelengths (see Fig. 3(b)). The gap between the straight and ring waveguides are 260 nm. A SiO_2 layer with the thickness of 1.5 μm is deposited as the cladding. After the waveguides are fabricated, TiN microheaters with the thickness of 150 nm are fabricated on the top of the MRRs. The aluminum trances with 50 μm in the width are formed to connect the pads and the microheaters.

In order to determine the working wavelengths of the device, an amplified spontaneous emission (ASE) source and an optical spectrum analyzer (OSA) are employed to measure the static response spectra of the device. The measured static response spectra with no voltage applied to the device is shown in Fig. 3(b). The insertion loss is about 5.3 dB which includes 5 dB coupling loss (about 2.5 dB for each end face) and 0.3 dB transmission loss, the extinction ratio for each MRR is similar (16.8 dB), and the resonant wavelengths of four cascaded MRRs are 1545.18 nm, 1548.10 nm, 1550.73 nm, and 1553.27 nm, respectively.

In fact, there are many different logic operations for the four operands. As proof of principle, only a few logic operations of four operands are demonstrated here. First, four MRRs are divided into two groups, and each group has two MRRs (see Fig. 4). The first group is composed of MRR_1 and MRR_2, and the wavelength of 1548.10 nm is chosen as the working wavelength λ_1. The second group is composed of MRR_3 and MRR_4, and the wavelength of 1553.27 nm is chosen as the working wavelength λ_2 (see Fig. 3(b)). The different operation modes of MRR are defined to perform different logic operations. For example, two lasers with the wavelengths of λ_1 and λ_2 are coupled into the input port of the device simultaneously, if the MRR_1 is controlled by operand A in the *pass/block* mode and the MRR_2 is controlled by operand B in the *block/pass* mode; the MRR_3 is controlled by operand C in the *block/pass* mode and the MRR_4 is controlled by operand D in the *block/pass* mode. Based on the above discussion, the device can perform the logic operation of $\bar{A}B + CD$ (see Fig. 4(a)). Similarly, other logic operations can also be achieved based on different operation modes of MRRs, and several examples are shown in Fig. 4.

3. Results

The measured dynamic response results of the device are shown in Fig. 5. Continuous lightwaves with the wavelengths of 1548.10 nm and 1553.27 nm from a two-channel tunable laser are simultaneously coupled into the device through a 2 $\times$ 1 combiner. Four binary sequences non-return-to-zero signals at 10 kbps generated by a four-channel signal source are applied to MRR_1, MRR_2, MRR_3 and MRR_4, respectively. Four MRRs are firstly divided into two groups. The first group includes MRR_1 and MRR_2, and its working wavelength is 1548.10 nm. The second group includes MRR_3 and MRR_4, and its working wavelength is 1553.27 nm. For the logic operation of $\bar{A}B + CD$, the high levels are 2.98 V and 2 V for MRR_1 and MRR_2; the low levels are 1.98 V and 0 V for MRR_1 and MRR_2, respectively. The high levels are 2.77 V and 2 V for

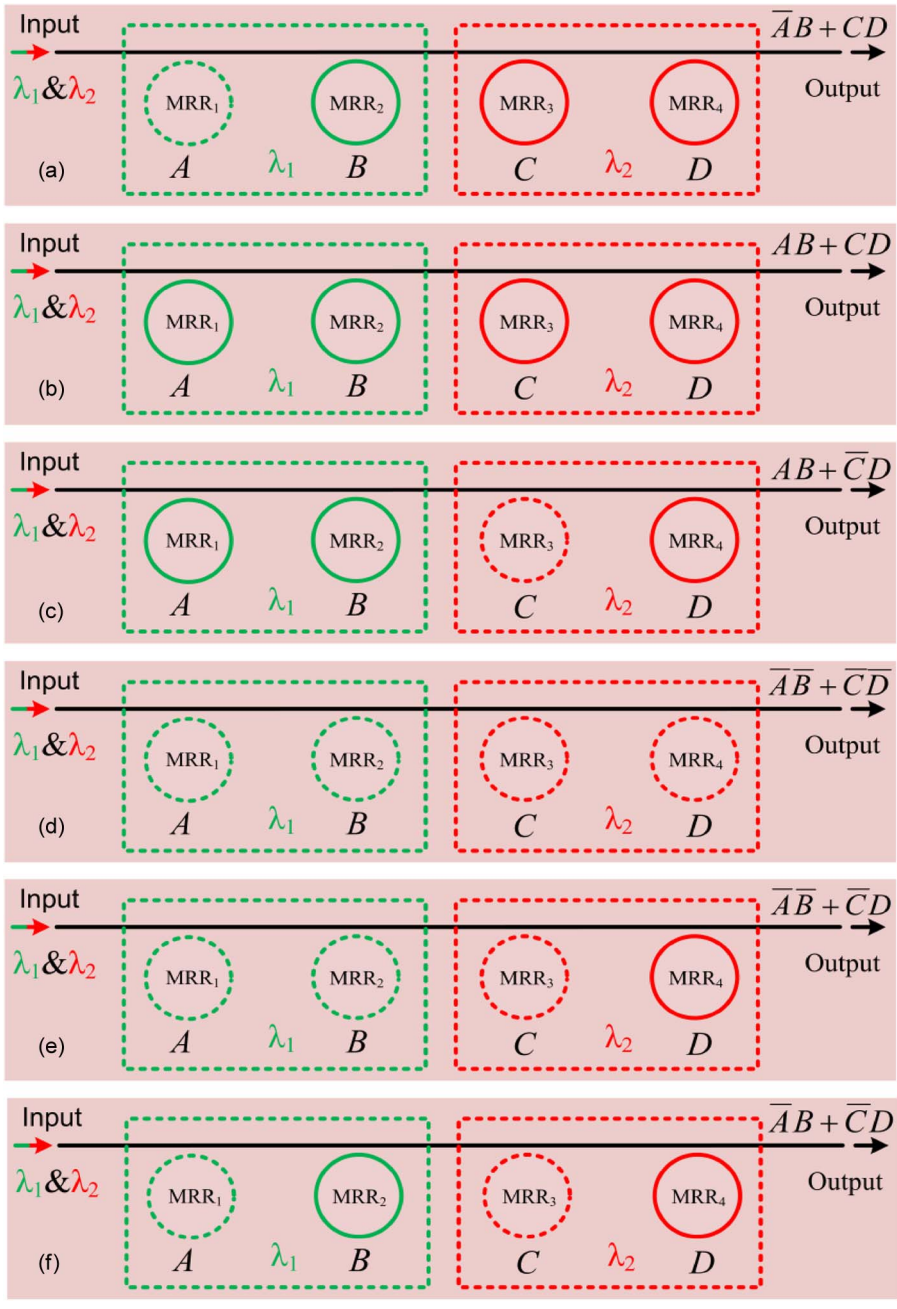

Fig. 4. Logic circuit diagrams of the device for different four-input logic operations (the solid line ring denotes MRR works in the block/pass mode; the dot line ring denotes MRR works in the pass/block mode, and MRRs with the same color work at the same working wavelength).

MRR_3 and MRR_4; the low levels are 1.77 V and 0 V for MRR_3 and MRR_4, respectively. Due to the fact that the modulation scheme is based on thermo-optic effect, the resistor is insensitive to the voltage polarity. Therefore, we can change MRRs' operation mode through the alteration of voltage polarity of pulse sequence applied to MRRs to achieve other different logic operations. For example, the high and low levels of pulse sequence applied to MRR_1 are inversed to be 1.98 and −2.98 V, respectively, and the other voltages are unchanged for other MRRs (in fact, the operation mode of MRR_1 has been changed from the *pass/block* mode to the *block/pass* mode in this case). In this case, the device can perform the logic operation of $AB + CD$ (see Fig. 5(f)).

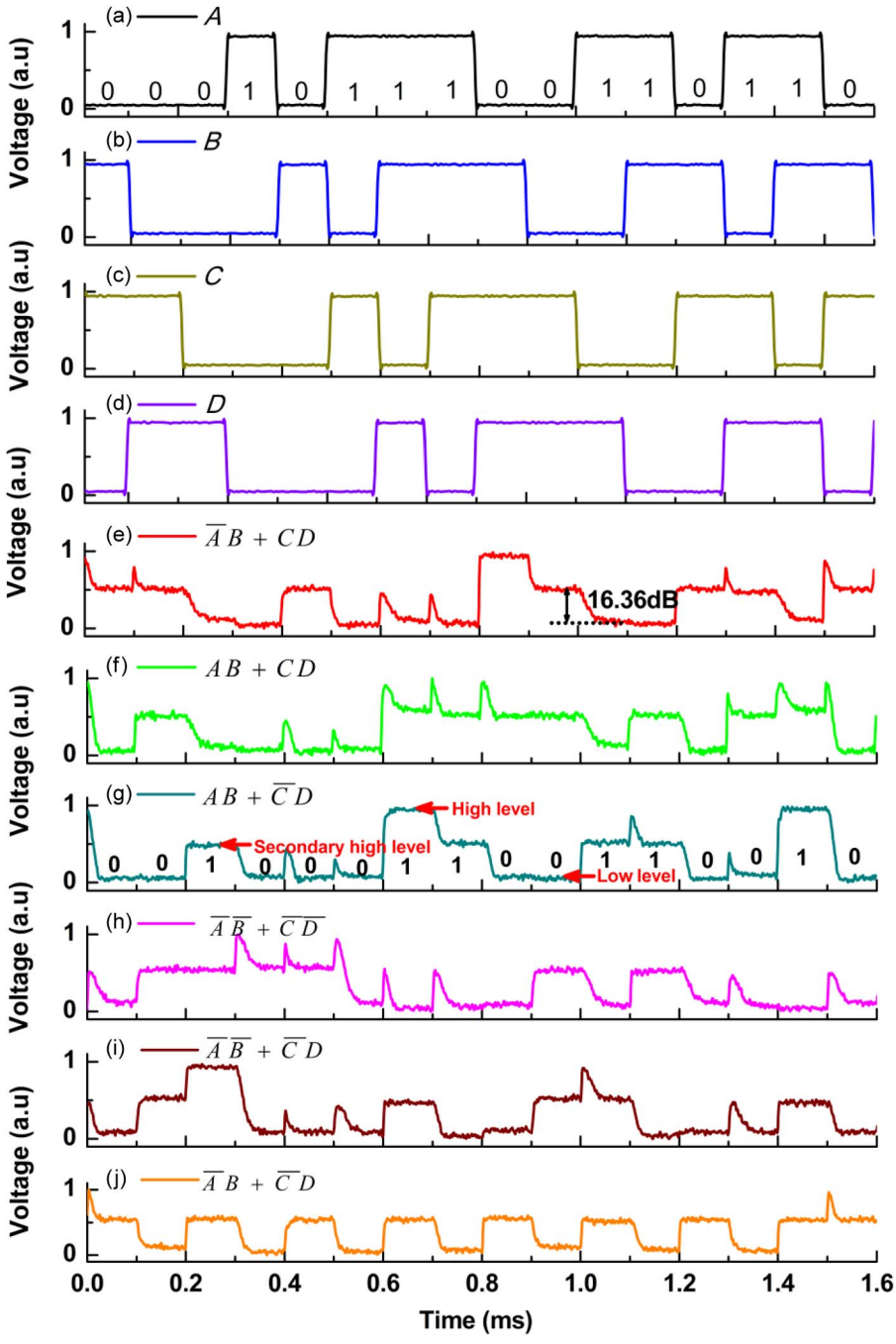

Fig. 5. Logic operation results of the device with four-operand ((a)–(d) represent the operands applied to MRRs, and (e)–(j) represent the logic operation results).

Similarly, the device can perform other logic operations through the alteration of voltage polarity (see Fig. 5(g)–(j)). The output light is transformed to the electrical signal by a photodetector (PD). The output electrical signal transformed by PD is fed into an oscilloscope for waveform observation. Clearly, the device can implement any logic operations which include two terms and every term is composed of the product of two operands (see Fig. 5). The device can implement any other four-operand logic operations through the alteration of the working wavelength numbers and the operation modes of optical switches (MRRs). Therefore, the proposed logic

circuit can perform reconfigurable logic operation based on WDM technology. Note that the high levels of the results are different due to the employing of WDM technology. However, it does not affect the performance of the device since we can also define the secondary high level as logic 1 (see Fig. 5(g)). The lowest dynamic extinction ratio is about 16.36 dB which is high enough to distinguish logic 1 and logic 0 in the field of digital communication (see Fig. 5(e)). In addition, some undesired small spikes can be found in Fig. 5 due to the alteration of working status for the device, which have been given detailed explanations in our previous works [6]. For a proof of principle, we only demonstrate several logic operations with four operands, and any other logic operations can also be implemented based on the similar principle. The operation speed is 10kbps due to the thermo-optic modulation scheme. However, other advanced modulating schemes such as the carrier-injection modulation, the carrier-depletion modulation and the electric field effects can also be employed to modulate the MRRs to achieve the higher speed operation of the device [13]–[17].

4. Conclusion

In conclusion, we propose a reconfigurable electro-optic logic circuit which can implement any logic operations based on MRR-based optical switch array. As a proof of principle, a four-input reconfigurable logic circuit based on four cascaded optical switches is fabricated, and several logic operations of four-operand with the operation speed of 10 kbps are demonstrated successfully.

References

[1] J. Hardy and J. Shamir, "Optics inspired logic architecture," *Opt. Exp.*, vol. 15, no. 1, pp. 150–165, Jan. 2007.
[2] H. J. Caulfield and S. Dolev, "Why future supercomputing requires optics," *Nature Photon.*, vol. 4, no. 5, pp. 261–263, May 2010.
[3] H. J. Caufslfield, R. A. Soref, and C. S. Vikram, "Universal reconfigurable optical logic with silicon-on-insulator resonant structures," *Photon. Nanostruct. Fundam. Appl.*, vol. 5, no. 1, pp. 14–20, Oct. 2007.
[4] J. Shamir, H. J. Caulfield, W. Micelli, and R. J. Seymour, "Optical computing and the Fredkin gates," *Appl. Opt.*, vol. 25, no. 10, pp. 1604–1607, May 1986.
[5] A. I. Zavalin, H. J. Caulfield, and C. S. Vikram, "Implementing minimal clock skew directed logic," *Optik, Int. J. Light Electron Opt.*, vol. 121, no. 14, pp. 1300–1308, Aug. 2010.
[6] L. Zhang *et al.*, "Demonstration of directed XOR/XNOR logic gates using two cascaded microring resonators," *Opt. Lett.*, vol. 35, no. 10, pp. 1620–1622, May 2010.
[7] Y. H. Tian *et al.*, "Proof of concept of directed OR/NOR and AND/NAND logic circuit consisting of two parallel microring resonators," *Opt. Lett.*, vol. 36, no. 9, pp. 1650–1652, May 2011.
[8] L. Zhang *et al.*, "Simultaneous implementation of XOR and XNOR operations using a directed logic circuit based on two microring resonators," *Opt. Exp.*, vol. 19, no. 7, pp. 6524–6540, Mar. 2011.
[9] L. Yang, L. Zhang, C. M. Guo, and J. F. Ding, "XOR and XNOR operations at 12.5 Gb/s using cascaded carrier-depletion microring resonators," *Opt. Exp.*, vol. 22, no. 3, pp. 2996–3012, Feb. 2014.
[10] Q. Xu and R. Soref, "Reconfigurable optical directed-logic circuits using microresonator-based optical switches," *Opt. Exp.*, vol. 19, no. 6, pp. 5244–5259, Mar. 2011.
[11] C. Y. Qiu, X. Ye, R. Soref, L. Yang, and Q. F. Xu, "Demonstration of reconfigurable electro-optical logic with silicon photonic integrated circuits," *Opt. Lett.*, vol. 37, no. 19, pp. 3942–3944, Oct. 2012.
[12] W. Mathlouthi, H. S. Rong, and M. Paniccia, "Characterization of efficient wavelength conversion by four-wave mixing in sub-micron silicon waveguides," *Opt. Exp.*, vol. 16, no. 21, pp. 16735–16745, Oct. 2008.
[13] A. S. Liu *et al.*, "High-speed optical modulation based on carrier depletion in a silicon waveguide," *Opt. Exp.*, vol. 15, no. 2, pp. 660–668, Jan. 2007.
[14] S. Feng, X. Luo, S. Du, and A. W. Poon, "Electro-optical tunable time delay and advance in a silicon feedback-microring resonator," *Opt. Lett.*, vol. 36, no. 7, pp. 1278–1280, Apr. 2011.
[15] M. Hochberg *et al.*, "Terahertz all-optical modulation in a silicon-polymer hybrid system," *Nature Mater.*, vol. 5, no. 9, pp. 703–709, Sep. 2006.
[16] C. Koos *et al.*, "All-optical high-speed signal processing with silicon-organic hybrid slot waveguides," *Nature Photon.*, vol. 3, no. 4, pp. 216–219, Apr. 2009.
[17] J. F. Ding *et al.*, "Ultra-low-power carrier-depletion Mach–Zehnder silicon optical modulator," *Opt. Exp.*, vol. 20, no. 7, pp. 7081–7087, Mar. 2012.